

Structure and photoluminescence properties of Ba₂TiSi₂O₈ glass ceramics prepared by aerodynamic levitation

Sang-Kyo Jung, Won-Seung Cho and Chi-Hwan Lee*

School of Materials Science and Engineering, Inha University, 253 Yonghyun-Dong, Nam-Gu, Incheon 402-751, Korea

Spherical Ba₂TiSi₂O₈ (BTS) and Dy³⁺-doped BTS glass were prepared by aerodynamic levitation. The glass prepared by aerodynamic levitation demonstrated enhanced glass stability. The crystallization rate of the levitated sample was slower than that of the conventional melt-quenched glass. When the heat treatment temperature was increased, the lattice parameter, *a*, of the nanocrystalline BTS crystal formed in the glass decreased, but the lattice parameter, *c*, increased. This was mainly due to the crystallization-induced stress during the crystallization process. Nanocrystallized Dy³⁺-doped BTS glass exhibited yellow (575 nm), red (669 nm), and blue (484 nm) luminescence. The intensities of all emission peaks increased with increasing heat-treatment temperature due to the increased crystallization of BTS crystals. Nanocrystallized BTS glass ceramic prepared by aerodynamic levitation is potentially useful for optical devices, such as visible semiconductor lasers, optical switches, and amplifiers.

Key words: Aerodynamic levitation, Ba₂TiSi₂O₈ glass, Photoluminescence, Microstructure, Crystallization.

Introduction

Fresnoite (Ba₂TiSi₂O₈, BTS) exhibits blue-white luminescence even without activator [1]. BTS crystals also show pyroelectric [2], ferroelectric [3], piezoelectric [4, 5], fluorescence [1, 6], and non-linear optical properties [7].

Photoluminescence (PL) of rare-earth (RE) ions in glassy or crystalline solids is one of the fundamental light-matter interactions, and has been utilized for various photonic devices. Dy³⁺ ions in solids yield yellow (~ 570 nm) emissions resulting from the f-f transition of ⁴F_{9/2} → ⁶H_{13/2} and 1.3 μm emissions due to the ⁶F_{11/2}, ⁶H_{9/2} → ⁶H_{15/2} transition. These emissions have been considered for visible solid-state lasers and optical amplifiers in broad band telecommunication systems [8]. Those Dy³⁺-doped phosphors have the important role of producing white light from UV light emission diodes [9] whose yellow/blue ratio can be tuned by distortions in the matrix [10].

On the other hand, nanostructures are the gateway into a new realm in physical, chemical, biological, and materials science. Crystallization of glass is an effective new method for nanostructure fabrication [11], and, recently, new optically transparent bulk nanocrystallized glasses (glass-ceramics) have been successfully fabricated [12-15]. Among these, transparent nanocrystallized glass consisting of nonlinear optical/ferroelectric nanocrystals has received a great deal of attention, because such materials have

considerable potential for applications in photonic devices such as tunable waveguides and optical switching [16, 17]. In RE-doped nonlinear optical/ferroelectric crystals, laser emissions in the short-wavelength region have been expected through self-frequency doubling (SFD) phenomena [18, 19].

The glass having a stoichiometric BTS composition, however, has an extremely high nucleation rate (~ 10¹⁷ m⁻³ s⁻¹) [19] that indicates an extremely high tendency of phase separation. The interface of phase separation is thermodynamically unstable. As the interface can act as a nucleation site, the conventionally-melted BTS glass demonstrates an extremely high nucleation rate [20].

Recently, containerless levitation techniques have been developed that will avoid chemical contamination and heterogeneous nucleation from the container wall. Levitation techniques can be utilized for the development of a new functional amorphous phase.

Therefore, in this study, spherical Ba₂TiSi₂O₈ (BTS) and Dy³⁺-doped BTS glass were prepared by aerodynamic levitation. In order to fabricate nanocrystallized BTS glass showing excellent optical properties, the effect of heat-treatment temperature on the microstructure and photoluminescence characteristics were also carefully investigated. For comparison, the BTS and Dy³⁺-doped BTS glass were prepared by melting at 1550 °C for 1 h and quenching using a conventional glass-making (melt-quenching) process.

Experimental Procedure

Sample preparation

Glass compositions of 40BaO-20TiO₂-40SiO₂ (mol%) and 40BaO-20TiO₂-40SiO₂-0.5Dy₂O₃ (mol%)

*Corresponding author:
Tel : +82-32-860-7538
Fax : +82-32-862-5546
E-mail: inhalee@inha.ac.kr

were prepared. The following raw materials were used: BaCO₃ (Duksan Pure Chemical, Co., LTD., Korea), TiO₂ (99.9%, High Purity Chemicals Co., LTD., Japan), SiO₂ (99.99%, High Purity Chemicals Co., LTD., Japan), and Dy₂O₃ (99.9%, Shin-Etsu Chemical Co., LTD., Japan). The powders were ball-milled for 24 h in an ethanol medium using a plastic jar with ZrO₂ balls. The slurries were dried simultaneously using a rotary evaporator. The glass batch was poured into a Pt crucible (50 ml) and kept at 800 °C for 30 min to remove CO₂ due to the decomposition of BaCO₃ (BaCO₃(s)BaO(s) + CO₂(g)). Finally, the glass batch was melted at 1550 °C for 1 h. Then, for vitrification, the melt was quenched on a graphite plate and maintained at 20 °C.

A spherical sample with a 2.5 mm diameter was levitated by an aerodynamic levitator using O₂ gas at a flow rate of 400 ml/min. The flow rate of the floating gas was controlled by a mass flow controller. The spherical sample was heated and melted under radiation of a CO₂ laser (Firestar-t series, Synrad Inc., USA) with a power output of 40–45 W. The surface temperature of the levitated droplet was monitored by a two-color pyrometer (Chino IRFBWWHSP, Chino Corp., Tokyo, Japan) at a sampling rate of 100 Hz and a spot size diameter of 1 mm. The response time of the pyrometer was 2.0 ms and the measurement error was ~0.5% of the as-measured temperature. The droplet was subsequently cooled by turning off the CO₂ laser. A high-speed video (HSV) camera (FASTCAM R2, Photron Inc., USA) was used to observe solidification on the droplet surface during cooling with an acquisition rate of 1,000 Hz.

Property measurement

The samples were crushed and ground using an agate mortar and pestle. The powdered material was used for differential scanning calorimetry (DSC) analysis experiments, as well as x-ray diffraction (XRD) analysis.

The crystalline structure of the samples was analyzed via XRD studies (DMAX-2500, Rigaku) using Cu K α radiation in the 2 θ range, 10°–90°, and at a scanning rate of 0.5°/min. The lattice parameters of the tetragonal phases were calculated from the XRD patterns using Nelson-Riley extrapolation [21]. The glass transition and crystallization temperatures were estimated using

DSC (404 F1, NETZSCH). In the DSC analysis, the powdered samples were put into a Pt crucible and heated from room temperature to 1450 °C at a heating rate of 10 °C/min in air.

BTS glass was heat treated for 1 h in air at a temperature range between the glass transition temperature (T_g) and crystallization onset temperature (T_x). The heat treatment temperature range for levitated and conventional melt-quenched glass was 720 to 750 °C and 710 to 740 °C, respectively.

The crystallinity of BTS glass as a function of heat treatment temperature was calculated from the XRD peaks using the following equation:

$$\text{Percentage of crystallinity} = \frac{\sum A_c}{\sum A_c + \sum A_a} \times 100(\%)$$

where $\sum A_c$ is the sum of the areas under all the crystalline peaks and $\sum A_a$ is the sum of the area under the amorphous peak.

Photoluminescence measured at room temperature using a photoluminescence spectrometer (SPEX 1403, SPEX). A He-Cd laser (55 mW) with a wavelength of 325 nm was used as an excitation source.

Results and Discussion

Fig. 1 shows the temperature-time profile for Dy³⁺-doped BTS glass during levitation. The Dy³⁺-doped BTS glass was kept at 1712 °C for 30 s and then cooled. The

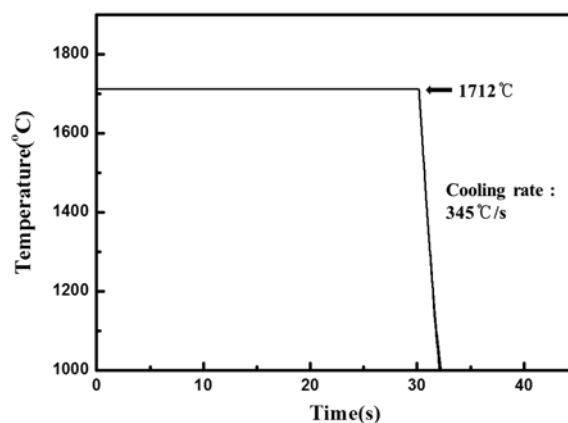


Fig. 1. Typical temperature-time profile for Dy³⁺-doped BTS glass during aerodynamic levitation.

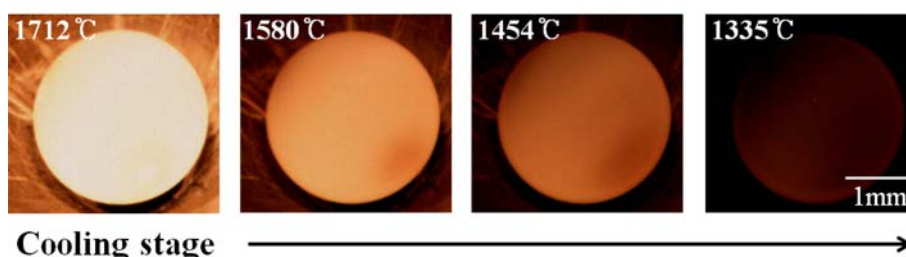


Fig. 2. Images of BTS droplets during cooling.

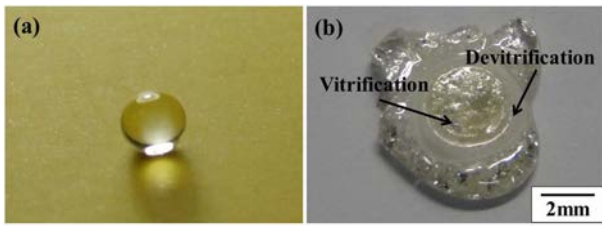


Fig. 3. Photographs for BTS glasses prepared via (a) an aerodynamic levitation technique and (b) the conventional melt-quenching process.

sample was continuously cooled to ambient temperature without recalescence, as frequently observed during solidification of crystalline ceramics. The cooling rate over a temperature range from 1712 °C to 1000 °C was 345 °C/s.

Fig. 2 shows images of a BTS molten droplet during cooling, as recorded on a color HSV camera. It was evident that the molten droplet was continuously cooled to ambient temperature.

Fig. 3 shows photographs for BTS glass-ceramics prepared by an aerodynamic levitation technique. Photographs of the BTS glass prepared by conventional melt-quenching are also given for comparison.

An almost spherical BTS glass with a diameter of 2.5 mm was fabricated by the containerless levitation technique. The appearance of the levitated sample was transparent, implying an amorphous phase. As mentioned above, the levitation process can prevent heterogeneous nucleation during containerless solidification, thereby enhancing vitrification. In contrast, the conventional melt-quenched sample consisted of transparent and translucent regions. Some regions of the sample were devitrified by crystallization during quenching on the graphite plate. Crystallization of the glass is likely to occur at the glass surface, because the surface acts as a heterogeneous nucleation site. Hereafter, the DSC and XRD experiments were conducted for the vitrified region of the conventional melt-quenched BTS glass.

Fig. 4 shows the DSC analyses results of BTS and Dy³⁺-doped BTS glass prepared by levitation and conventional melt-quenching. From the DSC curves, the glass transition (T_g), crystallization onset (T_x), crystallization peak (T_p), and melting temperatures (T_m) were estimated. The T_g , T_x , T_p , and T_m for BTS glass

are listed in Table 1.

In levitated samples, the values of T_g , T_x , T_p and T_m for the BTS glass are 709 °C, 787 °C, 807 °C, and 1432 °C, respectively. The corresponding values for the Dy³⁺-doped BTS glass are 714 °C, 797 °C, 815 °C, and 1415 °C. In the conventional melt-quenched samples, the values of T_g , T_x , T_p , and T_m for BTS glass-ceramic are 707 °C, 780 °C, 803 °C, and 1433 °C, respectively. The corresponding values for the Dy³⁺-doped BTS glass are 713 °C, 790 °C, 814 °C, and 1424 °C.

With the addition of Dy³⁺ ions, T_g , T_x and T_p increased slightly. This indicates improved glass stability for the Dy³⁺-doped BTS glass.

Hrubý proposed that a parameter, K_H , obtained by differential thermal analysis (DTA) or DSC, indicates glass stability against crystallization upon heating [22].

The Hrubý parameter is defined by

$$K_H = \frac{T_x - T_g}{T_m - T_x}$$

where T_x , T_g and T_m are the onset crystallization temperature (on heating), glass transition and melting temperatures estimated by DSC, respectively. According to Hrubý, a higher K_H value of a certain glass suggests a greater stability against crystallization upon heating, and higher vitrifiability during cooling [22]. In this study, the levitated samples BTS glass and Dy³⁺-doped BTS glass had K_H values of 0.12 and 0.13, respectively. These values are slightly higher than conventional melt-quenched samples (0.11 for BTS glass-ceramic and 0.12 for Dy³⁺-doped BTS glass-ceramic).

As the typical K_H values of glass range between 0.1 and 2 [22], the $K_H = 0.11$ -0.13 values calculated in this study indicated a higher tendency of the BTS glass to crystallize than typical glass.

The improvement in glass stability was thought to be due to the improved glass structure connection and obtaining a higher band polymerization degree by increasing the cation field strength (CFS) value [23]. The CFS value increased when a trivalent rare earth ion (Dy³⁺) was substituted at the Ba²⁺ site. (ionic radius: 0.143 nm for Ba²⁺ and 0.107 nm for Dy³⁺ [24]),

$$CFS = \frac{\text{Valence}}{(\text{Ionic radius})^2}$$

Fig. 5 shows the changes in transparency for the

Table 1. Glass transition temperature (T_g), crystallization onset temperature (T_x), crystallization peak temperature (T_p) and melting point (T_m) of levitated BTS and Dy³⁺-doped BTS glass. The corresponding data for BTS and Dy³⁺-doped BTS glass prepared via a conventional fabrication process are shown for comparison.

Process	Sample	T_g (°C)	T_x (°C)	T_p (°C)	T_m (°C)	K_H [($T_x - T_g$)/($T_m - T_x$)]
Levitated	BTS	709	787	807	1432	0.12
	Dy ³⁺ -doped BTS	714	797	815	1415	0.13
Conventional melt-quenched	BTS	707	780	803	1433	0.11
	Dy ³⁺ -doped BTS	713	790	814	1424	0.12

Dy³⁺-doped BTS levitation sample according to the heat treatment temperature. The appearance of the levitated sample changes from transparent to translucent at temperatures higher than 740 °C. This was ascribed to the devitrification by crystallization.

Fig. 6 shows the XRD patterns of the levitated (a) BTS and (b) Dy³⁺-doped BTS glass as a function of heat treatment temperature. Each sample was heated over a temperature range between T_g and T_x , and held for 1 h at the desired temperature. In all samples, irrespective of Dy³⁺ doping, broad humps were observed at $\sim 27^\circ$ in both the as-levitated and heat-treated samples at 720 °C, which implies the presence of an amorphous phase. The tiny peaks corresponding to (201) and (211) planes, the main peaks of BTS, appeared upon heat-treating the BTS glass at 730 °C, implying the presence of tiny crystalline phases. All peaks corresponding to BTS were detected at temperatures higher than 740 °C. Crystallization occurred at temperatures higher than T_g (709 °C for BTS glass and 714 °C for Dy³⁺-doped BTS glass). It was noted that a small amount of amorphous phase still remained even after heat treatment at 750 °C for 1 h. Therefore, the percent crystallinity of BTS and Dy³⁺-doped BTS glass was calculated by measuring the areas under all crystalline peaks and the amorphous peak.

Fig. 7 shows the percent crystallinity of BTS and Dy³⁺-doped BTS glasses as a function of heat treatment temperature. The glass samples were held for 1 h at the

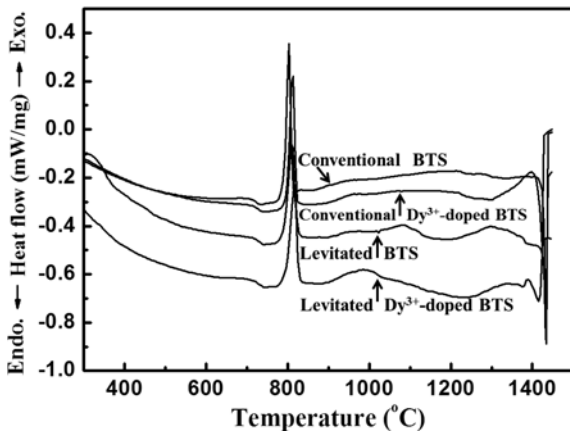


Fig. 4. DSC analyses for BTS and Dy³⁺-doped BTS glass. The glass was prepared by aerodynamic levitation and a conventional fabrication process.

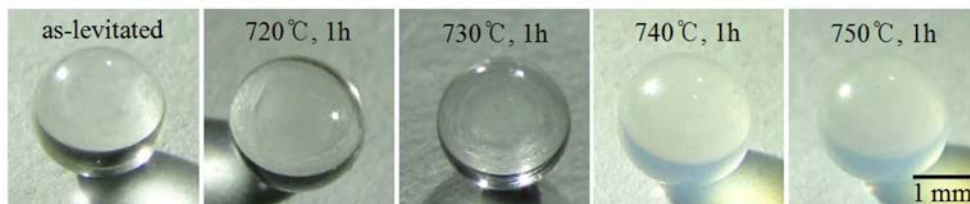


Fig. 5. Change in transparency of Dy³⁺-doped BTS levitation samples with heat treatment temperature. The optical transparencies of the levitated sample changes from transparent to translucent based on heat treatment at a temperature higher than 740 °C.

heat treatment temperature. The crystallinity increased with heat treatment temperature. The crystallinity of samples, prepared by a conventional fabrication process, was also presented for comparison. The conventionally melt-quenched glass was rapidly crystallized with temperature, and almost crystallized at 740 °C. It is noteworthy that the crystallization rates of the levitated samples were slower than those in the conventionally melt-quenched glass. This result indicates the low tendency of crystallization in the levitated samples. The glass with a stoichiometric BTS composition indicates an extremely high tendency of phase separation [20]. The interface of phase separation is thermodynamically unstable. As the interface can act as a nucleation site, the

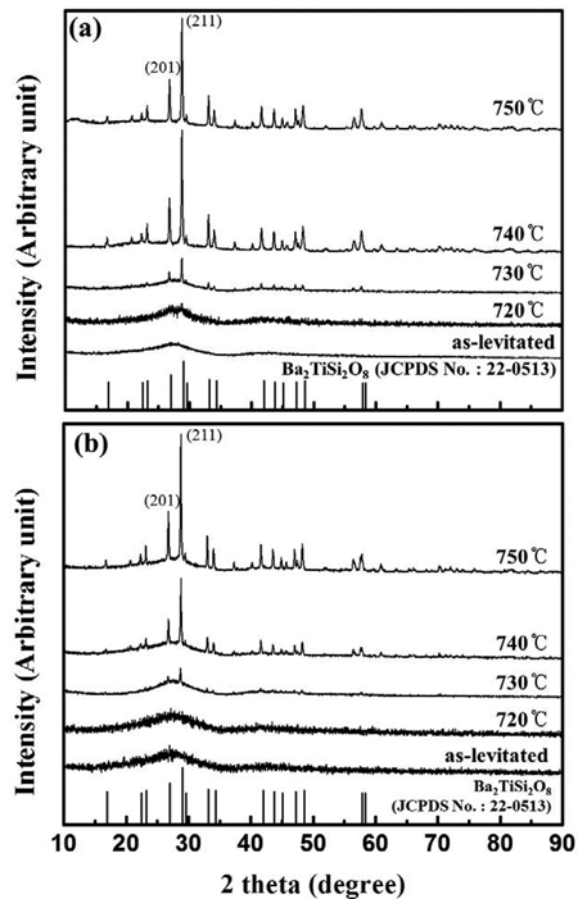


Fig. 6. XRD patterns for levitated (a) BTS and (b) Dy³⁺-doped BTS samples. Each sample was heated at the desired temperature for 1 h.

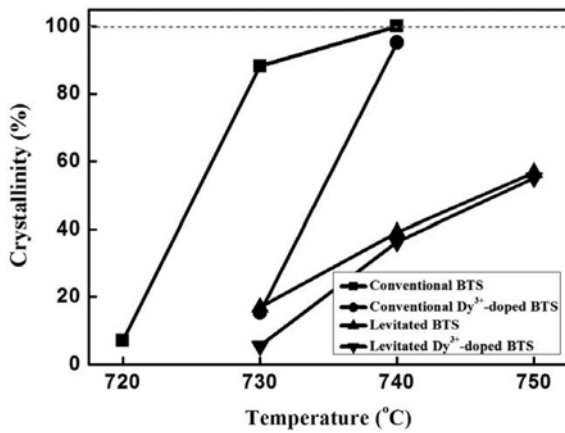


Fig. 7. Degree of crystallization for BTS and Dy^{3+} -doped BTS glasses as a function of heat treatment temperature. The glass was prepared by aerodynamic levitation and conventional fabrication processes, and then heat-treated for 1 h.

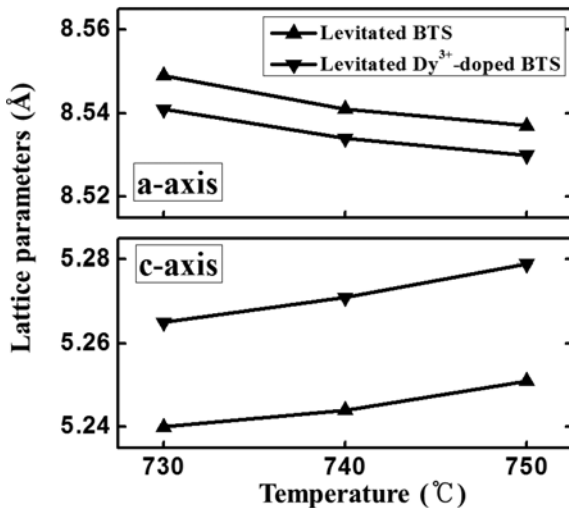


Fig. 8. Lattice parameters (a- and c-axis) for BTS and Dy^{3+} -doped BTS glass as a function of heat treatment temperature. The glass was prepared by aerodynamic levitation, and then heat-treated for 1 h.

conventionally melted BTS glass should demonstrate an extremely high nucleation rate. However, as the molten glass rapidly solidifies during levitation, the nucleation site is greatly decreased, resulting in decreased crystallization upon subsequent heat treatment. Thus, the levitated glass sample is expected to offer easier size and volume control of the nanocrystalline phase than the conventionally melted glass samples.

Fig. 8 shows the lattice parameters of BTS and Dy^{3+} -doped BTS glass, prepared by the levitation process, and then heat-treated at various temperatures for 1 h. It is proposed that Dy^{3+} ions substitute Ba^{2+} sites in BTS nanocrystals. (ionic radius: 0.143 nm for Ba^{2+} and 0.107 nm for Dy^{3+}). The lattice parameters were calculated using Nelson-Riley extrapolation. By increasing heat treatment temperature, the a-axis lattice parameters (a) decreased, whereas the c-axis lattice parameters (c)

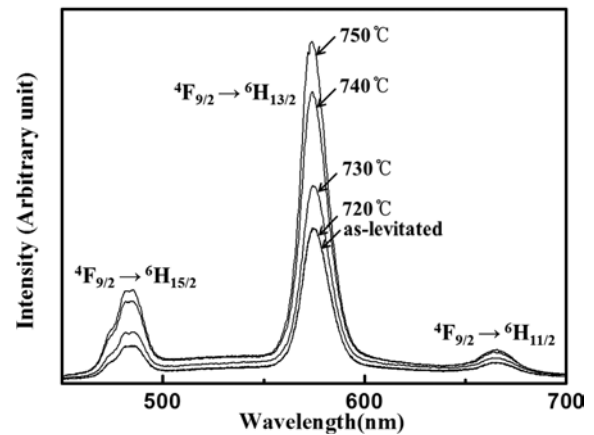


Fig. 9. Photoluminescence spectra for the as-levitated Dy^{3+} -doped BTS glass and Dy^{3+} -doped BTS crystallized glass.

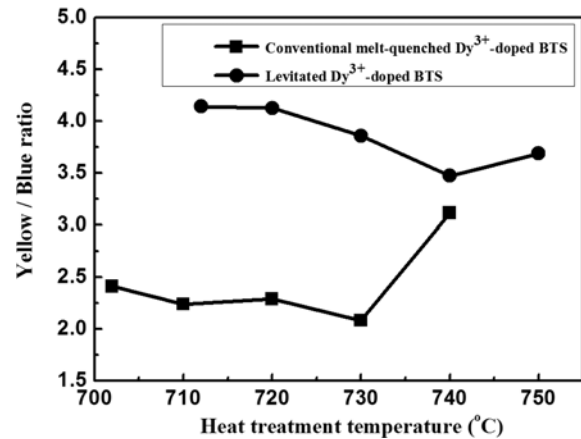


Fig. 10. The yellow/blue intensity ratios for the levitated and conventional melt-quenched Dy^{3+} -doped BTS glass.

increased.

The linear expansion coefficient of the parent glass (α_g) was $8.5 \times 10^{-6} \text{C}^{-1}$ [25] and that of the BTS crystal was $5.7 \times 10^{-6} \text{C}^{-1}$ (α_a) and $9.9 \times 10^{-6} \text{C}^{-1}$ (α_c) [26]. In the case of cooling of the BTS glass-ceramic, compressive stress is created along the a-axis direction because α_a is smaller than α_g , while tensile stress is created along the c-axis direction because α_c is larger than α_g . Thus, the cooling of crystallized glass (or glass-ceramic) to room temperature entails contraction or expansion of the lattice parameters. However, the change in the lattice parameter along the a-axis is smaller than the change in the lattice parameter along c-axis, even though the thermal expansion mismatch along the a-axis is much greater. Furthermore, the large change in lattice parameters at temperature ranges of 730–750 °C could not be explained because the estimated thermal strain is too small. The large change in lattice parameters could be caused by crystallization-induced stress rather than thermal stress. Ochi reported that the difference in density between the parent BTS glass (4.05 g/cm^3) and the fresnoite crystal (4.43 g/cm^3) contributes to the crystallization-induced stress [25].

Ochi reported that residual stress resulting from the crystallization process applies a compression force to the layers composed of TiO_5 square pyramids and SiO_2 tetrahedra in the direction normal to the *c*-axis. As a consequence, the layers expand in the direction of the *c*-axis. Therefore, the change in lattice parameters was mainly ascribed to crystallization-induced stress formed during the crystallization process.

Fig. 9 shows the photoluminescence (PL) spectra for Dy^{3+} -doped BTS glass and crystallized glasses, prepared by levitation process. Three peaks assigned to the f-f transitions of $^4\text{F}_{9/2} \rightarrow ^6\text{H}_{15/2}$ (blue: 484 nm), $^4\text{F}_{9/2} \rightarrow ^6\text{H}_{13/2}$ (yellow: 575 nm) and $^4\text{F}_{9/2} \rightarrow ^6\text{H}_{11/2}$ (red: 669 nm) are observed. The intensity of these peaks increased due to the crystallization. In particular, the crystallized samples showed a strong intensity at the peak corresponding to the $^4\text{F}_{9/2} \rightarrow ^6\text{H}_{13/2}$ transition (yellow emission) compared with the as-levitated BTS glass.

Fig. 10 shows the emission intensity ratio of the yellow ($^4\text{F}_{9/2} \rightarrow ^6\text{H}_{13/2}$ transition)/blue ($^4\text{F}_{9/2} \rightarrow ^6\text{H}_{15/2}$ transition) peaks, which were estimated from the spectra for Dy^{3+} -doped BTS glass prepared by levitation and conventional melt-quenching. The emission intensity ratio of conventional melt-quenched Dy^{3+} -doped BTS glass decreased slightly until 730°C, but increased at 740 °C. Levitated Dy^{3+} -doped BTS glass decreased slightly up to 740 °C, and then increased slightly at 750 °C. As shown previously in Fig. 7, the crystallinity of conventional melt-quenched Dy^{3+} -doped BTS glass was approximately 15% at 730 °C and increased rapidly up to 95% at 740°C. The crystallinity of levitated Dy^{3+} -doped BTS glass was approximately 36% at 740 °C and increased up to 55% at 750 °C. This result is consistent with the Judd-Ofelt analyses that the site symmetry of Dy^{3+} ions in the crystallized glass is largely distorted, yielding a large increase in yellow emissions [8]. This result was also consistent with the work of Maruyama *et al.* [8]. They proposed that Dy^{3+} ions substitute Ba^{2+} sites in BTS nanocrystals. Levitated Dy^{3+} -doped BTS glass demonstrated a higher emission intensity ratio than conventional melt-quenched Dy^{3+} -doped BTS glass, implying a large distortion in the site symmetry of Dy^{3+} ions.

Conclusions

Spherical $\text{Ba}_2\text{TiSi}_2\text{O}_8$ (BTS) and Dy^{3+} -doped BTS glass were prepared by aerodynamic levitation. The effects of heat-treatment temperature on the microstructure and photoluminescence characteristics were also investigated.

1. Spherical $\text{Ba}_2\text{TiSi}_2\text{O}_8$ (BTS) and Dy^{3+} -doped BTS glass were prepared by aerodynamic levitation. The glass prepared by aerodynamic levitation demonstrated enhanced glass stability. The crystallization rate of the levitated sample was slower than that of the conventional melt-quenched glass.

2. Upon increasing the heat treatment temperature, the lattice parameter, *a*, of nanocrystalline BTS crystal formed in glass decreased, but the lattice parameter, *c*, increased. This result was attributed to crystallization-induced stress that formed during the crystallization process.

3. Nanocrystallized Dy^{3+} -doped BTS glass exhibited yellow (575 nm), red (669 nm) and blue (484 nm) luminescence. With increasing heat-treatment temperature, the intensities of all emissions increased due to increased crystallization of the BTS crystals. Nanocrystallized BTS glass ceramic prepared by aerodynamic levitation is potentially useful for optical devices

Acknowledgments

This study was supported by the National Research Foundation of Korea funded by the Ministry of Education, Science and Technology (NRF-2012RIA1 A2008361) and a INHA UNIVERSITY Research Grant.

References

1. G. Blasse, and J. Inor, Nucl.Chem. 30, [8] (1968) 2283-84.
2. H. Yamauchi, K. Yamashita, and H. Takeuchi, J. Appl. Phys. 50 (1979) 3160-67.
3. M. C. Foster, D. J. Arbogast, R. M. Nielson, P. Photinos, and S. C. Abrahams, J. Appl. Phys. 85 (1999) 2299-2303.
4. M. Kimura, J. Appl. Phys. 48 (1977) 2850-56.
5. M. Kimura, Y. Fujino, and T. Kawamura, Appl. Phys. Lett. 29 (1976) 227-228.
6. Y. Takahashi, K. Kitamura, Y. Benino, T. Fujiwara, and T. Komatsu, Appl. Phys. Lett. 86 [091110] (1957) 7177-81.
7. P.S. Bechthold, S. Haussuehl, E. Michael, J. Eckstein, K.Recker, and F. Wallrafen, Phys. Lett. A 65 (1978) 453-54.
8. N. Maruyama, T. Honma, and T. Komatsu, J. Solid State Chem. 182 (2009) 246-252.
9. J. Pisarska, R. Lisiecki, W. Ryba-Romanowski, T. Goryczka, W.A. Pisarski, Chem. Phys. Lett. 489 (2010) 198-201.
10. L.L. Martin, P. Haro-González, I.R. Martín, Opt. Mater. 33 (2011) 738-741.
11. G.H. Beall, and L.R. Pinckney, J. Am. Ceram. Soc. 82 (1999) 5-16.
12. R. Sakai, Y. Benino, and T. Komatsu, Appl. Phys. Lett. 77 (2000) 2118-2120.
13. F. Torres, K. Narita, Y. Benino, T. Fujiwara, and T. Komatsu, J. Appl. Phys. 94 (2003) 5265-5272.
14. S. Prasad, K.B.R. Varma, Y. Takahashi, Y. Benino, T. Fujiwara, T. Komatsu, J. Solid State Chem. 173 (2003) 209-215.
15. Y. Takahashi, K. Kitamura, Y. Benino, T. Fujiwara, and T. Komatsu, Appl. Phys. Lett. 86 (2005) 091110-1-091110-3.
16. N. Iwafuchi, S. Mizuno, Y. Benino, T. Fujiwara, T. Komatsu, M. Koide, and K. Matusita, Adv. Mater. Res. 11-12 (2006) 209-212.
17. S. Mizuno, Y. Benino, T. Fujiwara, and T. Komatsu, Jpn. J. Appl. Phys. 45 (2006) 6121-6125.
18. J. Capmany, D. Jaque, J.G. Sole, and A. A. Kaminskii,

- Appl. Phys. Lett. 72 (1998) 531-533.
19. G. Aka, and A. Brenier, Opt. Mater. 22 (2003) 89-94.
20. A. A. Cabral, V. M. Fokin, E. D. Zanotto, and C.R. Chinaglia, J. Non-Cryst. Solids, 330 (2003) 174-186.
21. J. B. Nelson, and D. P. Riley, Proc. Phys. Soc. 57 (1945) 160-177.
22. A. Hruby, Czech. J. Phys. B, 22 (1972) 1187-1193.
23. Y.Cheng et al., Mater. Sci. Eng. A, 480 (2008) 56-61.
24. E. A. Brandes, and G. B. Brook, Smithells Metals Reference Book 7th edition, Butterworth-Heinemann Ltd (1992).
25. P. B. Moore, and S. J. Louisnathan, Zeitschrift für Kristallographie, Bd. 130, S (1969) 438-448
26. Y. Ochi, Mater. Res. Bull. 41 (2006) 740-750.
27. Tadzhiiev, Irkakhodzhaeva, and Sirazhiddinov, Handbook of Glass Data, C 0879, (1984).